Inorg. Chem. **2008**, *47*, 3128−3134

Inorganic Chemistry
Article

$SrAu_4In_4$ and $Sr_4Au_9In_{13}$: Polar Intermetallic Structures with Cations in Augmented Hexagonal Prismatic Environments

Andriy Palasyuk, Jing-Cao Dai,[†] and John D. Corbett*

Ames Laboratory−DOE and Department of Chemistry, Iowa State University, Ames, Iowa 50011

Received October 31, 2007

The title compounds were synthesized via high-temperature reactions of the elements in welded Ta tubes and characterized by single-crystal X-ray diffraction analyses and band structure calculations. $SrAu_{3.76(2)}In_{4.24}$ crystallizes in the YCo_5In_3 structure type with two of eight network sites occupied by mixtures of Au and In: *Pnma*, $Z = 4$, $a = 13.946(7)$, $b = 4.458(2)$, $c = 12.921(6)$ Å. Its phase breadth appears to be small. $Sr_4Au_9In_{13}$ exhibits a new structure type, $P\bar{6}m2$, $Z = 1$, $a = 12.701(2)$, $c = 4.4350(9)$ Å. The Sr atoms in both compounds center hexagonal prisms of nominally alternating In and Au atoms and also have nine augmenting (outer) Au + In atoms around their waists so as to define 21-vertex $Sr@Au_9M_4In_8$ (M = Au/In) and $Sr@Au_9In_{12}$ polyhedra, respectively. The relatively larger Sr content in the second phase also leads to condensation of some of the ideal building units into trefoil-like cages with edge-shared six-member rings. One overall driving force for the formation of these structures can be viewed as the need for each Sr cation to have as many close neighbors as possible in the more anionic Au−In network. The results also depend on the cation size as well as on the flexibility of the anionic network and an efficient intercluster condensation mode as all clusters are shared. Band structure calculations (LMTO-ASA) emphasize the greater strengths (overlap populations) of the Au−In bonds and confirm expectations that both compounds are metallic.

Introduction

Present systematic investigations of the Sr−Au−In system follow on explorations of the binary polar intermetallic phases formed between the triel elements (Tr = Al−Tl) and the electropositive alkali (A) or alkaline-earth (Ae) metals. These compounds are attractive because of their interesting structures, unexpected compositions, and novel bonding features, which usually deviate from classical valence models and Zintl concepts and challenge common concepts.[1−3] Alkali-metal−triel compounds contain relatively large proportions of cations and, often, discrete cluster anions, and application of classical bonding models to these is relatively easy, as in K_8In_{11},[4] $K_8In_{10}Zn$,[5] $Na_3K_8Tl_{13}$,[6] KNa_3In_9,[7] and $K_{34}Li_{12.7}In_{92.3}$.[8] The change to an alkaline-earth-metal−triel system usually generates more complex three-dimensional anionic networks that encapsulate smaller proportions of the cations, as in $BaIn_4$,[9] $SrIn_4$,[10] or Sr_3In_5,[11] and discrete polytrielide anions are no longer found. The complexities of these polyanions as well as their degrees of condensation appear to depend strongly on the charges of the cations as well as on their relative sizes and proportions.[10,12]

Additions of a third, electron-poorer transition metal with a nominal d^{10} shell, in particular, a late sixth period elements such as Au, greatly increase the number of new compounds and structures. Increases in the flexibility and in the variety of condensation modes for the polyanionic networks are evident, yet fairly regular structural motifs about the cations

---

* To whom correspondence should be addressed. E-mail: jdc@ameslab.gov.

[†] Current address: Institute of Materials Physical Chemistry, Huaqiao University, Quanzhou, Fujian 362021, China.

(1) (a) Nesper, R. *Angew. Chem., Int. Ed. Engl.* **1991**, *30*, 789. (b) Belin, C. H. E.; Tillard-Charbonnel, M. *Prog. Solid State Chem.* **1993**, *22*, 5.

(2) (a) Corbett, J. D. In *Chemistry, Structure and Bonding of Zintl Phases and Ions*; Kauzlarich, S. M., Ed.; VCH Publishers: New York, 1996; Chapter 4. (b) Corbett, J. D. *Angew. Chem., Int. Ed.* **2000**, *39*, 670.

(3) Miller, G. J.; Lee, C.-S.; Choe, W. In *Inorganic Chemistry Highlights*; Meyer, G., Naumann, D., Wesemann, L., Eds.; Wiley-VCH Verlag-Gmbh: Weinheim, Germany, 2002; Chapter 2.

(4) Sevov, S. C.; Corbett, J. D. *Inorg. Chem.* **1991**, *30*, 4875.

(5) Sevov, S. C.; Corbett, J. D. *Inorg. Chem.* **1993**, *32*, 1059.

(6) Dong, Z.-C.; Corbett, J. D. *J. Am. Chem. Soc.* **1995**, *117*, 6447.

(7) Li, B.; Corbett, J. D. *Inorg. Chem.* **2002**, *41*, 3944.

(8) Li, B.; Corbett, J. D. *J. Am. Chem. Soc.* **2005**, *127*, 926.

(9) Bruzzone, G. *Acta Crystallogr.* **1965**, *18*, 1081.

(10) Seo, D.-K.; Corbett, J. D. *J. Am. Chem. Soc.* **2000**, *122*, 9621.

(11) Seo, D.-K.; Corbett, J. D. *J. Am. Chem. Soc.* **2002**, *124*, 415.

(12) Li, B.; Corbett, J. D. *Inorg. Chem.* **2003**, *42*, 8768.

10.1021/ic702145y CCC: $40.75

are evident, namely, quite regular pentagonal or hexagonal prismatic environments but with diverse augmentations about the waists of these prisms. Significantly stronger bonding of the third element into the network is also evident, and notions about lattice stability, size matching, and optimal bonding of the cations within such three-dimensional networks become more important and complex than in systems with discrete clusters. Significant additional stabilities (Madelung energies) seem apparent because of distinctly more polar bonding of the triels to late 5d transition metals via their significant relativistic effects and, in turn, greater electonegativities.

These effects were first clearly noted in Ba_2AuTl_7,[13] $BaAuTr_3$ ($BaAl_4$ type, Tr = In, Tl),[14] $BaAu_xTr_{2-x}$,[15] as well as, at least implicitly, for $SrAu_2In_2$,[16] $BaPtIn_3$,[17] Sr_2Pt_2In,[18] $SrPtIn_4$,[19] $SrAuIn_3$,[20] and others.[21] Relativistic effects for gold etc. and the extreme electronegativities that result are clearly very important, serving, for example, to shorten network bond lengths and cell volumes on isomorphous substitution for In. Related salutary effects on the formation of numerous novel networks have been found recently in the K−Au−In etc. systems.[22,23]

Herein we report on two more examples with augmented hexagonal prismatic environments around the cations and new network arrays, $SrAu_{3.76(2)}In_{4.24}$ (hereafter termed $SrAu_4In_4$) and $Sr_4Au_9In_{13}$. These extend the number of Sr−Au−In phases beyond those examples noted above[16,20,21] and the structurally similar $Sr_2Au_3In_4$[24] and $SrAu_3In_3$.[25]

Experimental Section

Syntheses. The high purity reagents were dendritic Sr (99.9%, Alfa-Aesar), Au sheet (99.997%, Ames Laboratory), and In tear drops (99.99%, Alfa-Aesar). These were handled in N_2-filled gloveboxes in which the moisture levels were maintained below 0.1 ppm (volume). The surfaces of strontium and indium were cut clean with a scalpel just before use. The reactions were carried out in welded Ta metal tubing jacketed within evacuated fused silica containers and heated in resistance furnaces, as before.[4–10]

All reactions were run at 1000 °C for 24 h, then quenched in water, annealed at 800 °C for 120 h, and quenched again. Well-formed single crystals of $SrAu_4In_4$ and $Sr_4Au_9In_{13}$ were first obtained with at least 95% (no impurity lines) and about 60% (plus extra lines of $SrAuIn_3$ and $Sr_2Au_3In_4$) yields from the reactions with Sr/Au/In = 1:4:4 and 1:1.5:2.5, respectively. A substantially purer single phase of $Sr_4Au_9In_{13}$ was obtained in about 95% yield after the Sr/Au/In ratio was changed to 4:9:13, the refined stoichiometry. Judgements about phase purities in these cases were made on the basis of comparisons of the Guinier powder patterns with those calculated from the refined structures (illustrated in Supporting Information). It should be remembered that such a high yield synthesis of a material with a known structure furnishes powerful evidence for the analytical stoichiometry of the phase with the refined composition. (The formation of an X-ray amorphous product would negate this generality, of course.)

According to several loadings, we conclude that the structurally refined $SrAu_{3.76(2)}In_{4.24}$ (below) represents the Au-rich limit of the *Pnma* $SrAu_{3+x}In_{5-x}$ phase. The phase width appears to be relatively small; a synthesis from a gold-poorer 1:3.5:4.5 composition yielded an 80–85% pure sample of this YCo_5In_3-type phase with slightly larger cell dimensions (a = 14.075(4) Å, b = 4.458(2) Å, c = 12.950(5) Å, ΔV = 9.8(7) Å^3) plus a minor trace of an unidentified In-richer phase. The latter appeared to be almost pure (85–90%) after reaction of a 1:3:4 composition. Thus, the Au-poor limit of the solid solution $SrAu_{3+x}In_{5-x}$ must be slightly over $x = 0.5$.

Powder X-ray Diffraction. Powder diffraction data were collected with the aid of Huber 670 Guinier powder camera equipped with an area detector and Cu Kα radiation (=1.540598 Å). Powdered samples were homogeneously dispersed in a glovebox between two Mylar sheets with the aid of a little vacuum grease. These were in turn held between split Al rings that provided airtight seals. Unit cell parameters were refined using the WinXPow program.[26]

Structure Determinations. Single-crystal diffraction data sets were collected at 293(2) K with the aid of Mo Kα radiation and a Brucker SMART APEX CCD diffractometer, each in the form of three sets of 606 frames with 0.3° scans in ω and exposure times of 10 s per frame. The reflection intensities were integrated with the SAINT subprogram in the SMART software package.[27] The space group determination was done with the aid of XPREP program and the SHELXTL 6.1 software package.[28] The refinements proceeded successfully in the indicated centrosymmetric *Pnma* and $P\bar{6}$ space groups, respectively. (The latter was later upgraded, below.) Empirical absorption corrections for both compounds were made with the aid of the SADABS program.[29] Finally, each structure was solved by direct methods with the aid of SHELXTL 6.1 and refined by full-matrix least-squares on F_o^2, ultimately with anisotropic thermal parameters and a secondary extinction parameter.

For $SrAu_4In_4$, a few least-squares cycles of refinement of the indicated one Sr, three Au, and five In positions followed by a difference Fourier map revealed that In alone was too electron-poor for two sites according to their abnormally small displacement parameters (<0.004 Å^2) and refined occupancies (>100%). At this point $R1$ and the highest difference peaks were 0.066, 3.91 e•Å^{-3} (1.00 Å from Au1) and −5.15 e•Å^{-3} (0.70 Å from Au3), respectively. Allowing mixtures of gold and indium at the two former In sites, assuming no vacancies on these positions but with constraints on the positional and thermal parameters for the other atoms, gave more reasonable isotropic displacement parameters, small improvements in $R1$ (0.020), a largest residual peak of 3.85 e•Å^{-3}, and an altered composition of $SrAu_{3.76(2)}In_{4.24}$. The refine-

---

(13) Liu, S.; Corbett, J. D. *Inorg. Chem.* **2004**, *43*, 2471.
(14) Liu, S.; Corbett, J. D. *Inorg. Chem.* **2004**, *43*, 4988.
(15) Dai, J.-C.; Corbett, J. D. *Inorg. Chem.* **2006**, *45*, 2104.
(16) Dai, J.-C.; Corbett, J. D. *Inorg. Chem.* **2007**, *46*, 4592.
(17) Palasyuk, A.; Corbett, J. D. *Z. Anorg. Allg. Chem.* **2007**, *633*, 2563.
(18) Muts, I.; Nilges, T.; Rodewald, U. Ch.; Zaremba, V. I.; Pöttgen, R. *Z. Naturforsch. B* **2007**, *62*, 1563.
(19) Muts, I.; Zaremba, V. I.; Baran, V. V.; Pöttgen, R. *Z. Naturforsch. B* **2007**, *62*, 1407.
(20) Muts, I.; Pöttgen, R.; Zaremba, V. I. *Z. Anorg. Allg. Chem.* **2007**, *633*, 2591.
(21) Dai, J.-C.; Palasyuk, A.; Corbett, J. D. Unpublished research.
(22) Li, B.; Corbett, J. D. *J. Am. Chem. Soc.* **2006**, *128*, 12392.
(23) Li, B.; Corbett, J. D. *Inorg. Chem.* **2007**, *46*, 6022.
(24) Hoffmann, R.-D.; Pöttgen, R.; Rosenhahn, C.; Mosel, B. D.; Künnen, B.; Kotzyba, G. *J. Solid State Chem.* **1999**, *145*, 283.
(25) Muts, I. R.; Schappacher, F. M.; Hermes, W.; Zaremba, V. I.; Pöttgen, R. *J. Solid State Chem.* **2007**, *180*, 2202.
(26) *STOE WinXPow 2.10, STOE & Cie GmbH Hilpertstr*; Darmstadt, Germany, 2004.
(27) *SMART*; Bruker AXS, Inc.; Madison, WI, 1996.
(28) *SHELXTL*; Bruker AXS, Inc.; Madison, WI, 2000.
(29) Blessing, R. H. *Acta Crystallogr.* **1995**, *A51*, 33.

Table 1. Crystal and Refinement Data for $SrAu_{3.76(2)}In_{4.24}$ and $Sr_4Au_9In_{13}$

compounds	$SrAu_{3.76(2)}In_{4.24}$	$Sr_4Au_9In_{13}$
Fw	1314.85	3615.84
space group, *Z*	*Pnma* (No. 62), 4	$P\bar{6}m2$(No.187), 1
unit cell (Å), *a*	13.946(7)	12.701(2)
b	4.458(2)	-
c	12.921(6)	4.4350(9)
V (Å^3)	803.2(7)	619.6(2)
d_{calcd} (Mg/m^3)	10.873	9.691
μ, mm^{-1} (Mo Kα)	86.765	73.354
independent data/restraints/params	1059/0/58	615/0/36
goodness of fit on F^2	1.025	1.104
$R1/wR2$ [$I > 2\sigma(I)$]	0.0457/0.0939	0.0311/0.102
$R1/wR2$ (all data)	0.0621/0.0999	0.0371/0.105
largest diff. peak and hole (e·Å^{-3})	3.85, –4.66	3.22, –3.43

ment, finally with fixed site occupancies, anisotropic displacement parameters, and a secondary extinction correction, converged at $R1 = 0.046$, $wR2 = 0.094$ ($I > 2\sigma(I)$).

The structure of $Sr_4Au_9In_{13}$ was initially solved and refined in the indicated $P\bar{6}$ space group (two Sr in 1*e*, 3*k*, three Au in 3*j*, 3*j*, 3*k*, and four In in 3k, 1*c*, 3*j*, 3*j*, 3*k* positions) to $R1 = 0.043$, $wR2 = 0.080$ values ($I > 2\sigma(I)$). The largest residual peaks and holes in the ΔF map were 3.47 e·Å^{-3} (1.16 Å from In3) and $-$ 4.08 e·Å^{-3} (0.89 Å from Au1). However, visual inspection of the [001] projection showed that the two basic construction units might have symmetries higher than $\bar{6}$, namely, with three additional mirror planes perpendicular to the projection through the centers of each basic element. A further hint of the wrong space group was noticed in the doubled size isotropic equivalent displacement parameters (16:8) for one each of three basal Au and In atoms. The test for missing symmetry performed by PLATON[30] confirmed our suspicions and suggested space group $P\bar{6}m2$ as a correct one. This change gave more consistent isotropic displacement parameters and decreased *R*1 by 0.012. All positions were fully occupied by single atom types (1*e*, 3*k*, by Sr, 3*k*, 3*j*, 3*j*, by Au and 3*k*, 1*c*, 6*l*, 3*k* by In). Convergence occurred at $R1 = 0.031$, $wR2 = 0.102$ ($I > 2\sigma(I)$) with largest residual peak and hole in the ΔF map of 3.22 e·Å^{-3} (0.08 Å from Au2) and $-$ 3.43 e·Å^{-3} (0.79 Å from Au2), respectively. Some crystallographic data for each phase are summarized in Table 1, and the atom positions and important bond lengths are listed in Tables 2 and 3, respectively. More detailed crystallographic and refinement information as well as anisotropic displacement parameters are available in Supporting Information (cif).

Electronic Structure Calculations. In order to understand the chemical bonding in the structures better, tight binding electronic structure calculations were performed for both structures by linear-muffin-tin-orbital (LMTO) method in the atomic sphere approximation (ASA).[31] The radii of the Wigner–Seitz (WS) spheres were assigned automatically so that the overlapping potentials would be the best possible approximations to the full potentials, and no interstitial sphere was necessary with the default 16% overlap restriction.[32] The WS radii determined by this procedure were reasonable: in the nominal $SrAu_4In_4$, 2.29 Å for Sr, 1.59 Å for both Au1 and Au2, 1.57 Å for Au3, 1.74 Å for In1, 1.64 Å for both In2 and In3, 1.73 Å for In or Au on the M1 site and 1.66 Å for In on the M2 site, and in $Sr_4Au_9In_{13}$, 2.32 and 2.38 Å for Sr1 and Sr2, 1.58 Å for both Au1 and Au3, 1.53 Å for Au2, 1.64 Å and 1.56 Å for In1 and In2, and 1.56 Å for both In3 and In4.

Results and Discussion

Crystal Structures. The general view of $SrAu_{3.76(2)}In_{4.24}$ in Figure 1a, written as $SrAu_4In_4$ hereafter, illustrates its three-dimensional Au–In network, which is constructed from a single basic unit: a 21-vertex polyhedron centered by strontium, $Sr@Au_9M_4In_8$ (M = Au/In) (Figure 1b). This polyhedron can be described as a distorted hexagonal prism plus nine additional atoms in a distorted nonagon that is coplanar with Sr and lies about the waist, that is, a 6–9–6 arrangement of parallel planar rings. These stack along the *b* axis by sharing basal hexagonal faces. In the *ac* plane (Figure 1c), the nine-member ring of each polyhedron is seen to share five edges with two other coplanar nine-member rings plus three six-member rings of other neighboring polyhedra that are displaced by *b*/2. Bonds between layers are not shown for clarity. This and the arrangement in Figure 1a can be described in more detail in terms of zigzag chains of coplanar hexagonal prisms along *a* that are in turn stacked alternately along *c* with *b* = ¼ or ¾. Each Sr group thus has six Sr-centered neighboring prisms, two coplanar prisms that share outer rings and define the chains (above), and three in which pairs of the outer 9-ring atoms are inner atoms in neighboring hexagons, and vice versa. The last is a common model of augmentation in such structures. The sixth Sr–Sr relationship is different and more complex without ring sharing, but rather an overlapping pair with a step of *b*/2 appears as a group of three condensed triangles in Figure 2c.

The overall drive for the formation of such a complex structure can be interpreted as the need to give each Ae cation as many close neighbors as possible in the more anionic Au–In network. The principle was evidently first put forth for the monoclinic structure of $SrIn_4$,[10] and parallel interpretations have been given to orthorhombic $BaAu_2Tl_7$[13] and (Ba, Sr)Au_2In_2,[16] both of which occur in the same *Pnma* space group as here.

The ideal $SrAu_4In_4$ would be isotypic with that of YCo_5P_3[33] if atoms' identities are systematically altered as Y → Sr, Co → In and Au/In, and P → Au. The latter structure can naturally be described in terms of a 21-vertex polyhedra centered by yttrium with comparable polyhedral sharing. The present structure is also isotypic but not isostructural with that of $Ca_2Au_3In_4$[34] in which the In and Au occupy seven of the nine 4*c* sites and the remaining two positions are occupied by Ca. In $SrAu_4In_4$, one of these sites is filled by Sr and the second by In1. (A lower temperature monoclinic polytype of this composition is also known.[21]) Strikingly, no parallel examples have been reported for Ca or Ba that match any of the structurally similar 1:4:4, 1:3:3, 2:3:4, and 4:9:13 phases in the Sr–Au–In system, showing how critical size can be in the definition of such structures.

---

[30] Spek, A. L. *J. Appl. Crystallogr.* **2003**, *36*, 7.

[31] Tank, R.; Jepsen, O.; Burkhardt, A.; Andersen, O. K. *TB-LMTO-ASA Program*, version 4.7; Max-Plank-Institut für Festkörperforschung: Stutgart, Germany, 1995.

[32] Jepsen, O.; Andersen, O. K. *Z. Phys. B* **1995**, *97*, 35.

[33] Meisen, U. C.; Jeitschko, W. *J. Less-Common Met.* **1984**, *102*, 127.

[34] Hoffmann, D.-R.; Pöttgen, R. *Z. Anorg. Allg. Chem.* **1999**, *625*, 994.

Table 2. Atomic Coordinates, Isotropic Equivalent Displacement Parameters ($Å^2 \times 10^3$), and Sn/Au Site Occupancies[a] for $\mathrm{SrAu_{3.76(2)}In_{4.24}}$ and $\mathrm{Sr_4Au_9In_{13}}$

atom	Wyckoff position	symmetry	*x*	*y*	*z*	*U*(eq)	occ ≠ 1
$\mathrm{SrAu_{3.76(2)}In_{4.24}}$							
Sr	4*c*	*.m.*	0.2943(2)	1/4	0.8957(2)	15(1)	
Au1	4*c*	*.m*	0.1230(1)	1/4	0.5848(1)	15(1)	
Au2	4*c*	*.m*	0.1024(1)	1/4	0.2267(1)	18(1)	
Au3	4*c*	*.m*	0.3845(1)	1/4	0.3841(1)	21(1)	
In1	4*c*	*.m*	0.0259(1)	1/4	0.7795(1)	18(1)	
In2	4*c*	*.m*	0.0044(1)	1/4	0.4118(1)	13(1)	
In3	4*c*	*.m*	0.2997(1)	1/4	0.1952(1)	16(1)	
M1	4*c*	*.m*	0.0710(1)	1/4	0.0077(1)	23(1)	0.51(1) In
M2	4*c*	*.m*	0.3219(1)	1/4	0.5990(1)	17(1)	0.74(1) In
$\mathrm{Sr_4Au_9In_{13}}$							
Sr1	1*e*	$\bar{6}m2$	2/3	1/3	0	8(1)	
Sr2	3*k*	*mm*2	0.2061(3)	0.7939(2)	1/2	8(1)	
Au1	3*k*	*mm*2	0.7856(2)	0.2144(1)	1/2	7(1)	
Au2	3*j*	*mm*2	0.4540(1)	0.5460(1)	0	8(1)	
Au3	3*j*	*mm*2	0.0874(1)	0.9126(2)	0	10(1)	
In1	3*k*	*mm*2	0.5331(2)	0.4670(2)	1/2	7(1)	
In2	1c	$\bar{6}m2$	1/3	2/3	0	12(1)	
In3	6*l*	*m..*	0.3434(2)	0.2934(2)	0	8(1)	
In4	3*k*	*mm*2	0.1688(2)	0.8312(2)	1/2	11(1)	

[a] M sites were assumed to be fully occupied by In and Au, with the refined In fraction listed.

Table 3. Selected Bond Lengths (Å) and ICOHP Values (eV/bond) in $\mathrm{SrAu_{3.76(2)}In_{4.24}}$ and $\mathrm{Sr_4Au_9In_{13}}$

$\mathrm{SrAu_{3.76(2)}In_{4.24}}$						$\mathrm{Sr_4Au_9In_{13}}$		
bond	distance	−ICOHP[c,d]	bond	distance	−ICOHP[c,d]	bond	distance	−ICOHP
Au1−In1	2.856(2)	1.36	In2−In3	3.172(3)	0.70	Au1−In1	2.792(2)	1.67
Au1−In2	2.781(2)	1.70	In3−M2[a]	3.064(2)	0.93/0.94	Au1−In3[a]	2.862(2)	1.34
Au1−In2[a]	2.851(2)	1.40	M1−M1	2.987(2)	0.95/0.72	Au2−In1[a]	2.818(2)	1.58
Au1−In3[a]	2.857(2)	1.43	M1−M2[a]	2.932(2)	1.06/1.05	Au2−In2	2.654(2)	2.31
Au1−M2	2.780(2)	1.71	Sr−Au1	3.503(2)		Au2−In3	2.786(2)	1.62
Au2−In1[a]	2.859(2)	1.32	Sr−Au2	3.437(2)		Au3−In3	2.819(2)	1.61
Au2−In2	2.754(2)	1.82	Sr−Au3	3.347(2)		Au3−In4[a]	2.914(2)	1.26
Au2−In3	2.782(2)	1.59	Sr−In1[b]	3.944(2)		Au3−Au3	3.329(3)	0.43
Au2−M1	2.865(2)	1.16/1.00	Sr−In1[b]	4.033(3)		In1−In3[a]	3.204(2)	0.72
Au2−M2[a]	2.968(2)	1.03/1.02	Sr−In2	3.591(3)		In3−In3	3.092(4)	0.85
Au3−In1[a]	2.891(2)	1.19	Sr−In2[b]	3.844(2)		In3−In4[a]	3.316(3)	0.54
Au3−In3	2.712(2)	2.03	Sr−In3	3.660(2)		In4−In4	3.217(4)	0.72
Au3−M1[a]	2.811(1)	1.20/	Sr−In3[b]	3.871(3)		Sr1−Au1	3.430(2)	
Au3−M1	2.953(2)	0.94/	Sr−M1	3.807(2)		Sr1−In1	3.682(2)	
Au3−M2	2.911(2)	1.19/1.17	Sr−M1[b]	3.434(3)		Sr1−In3[b]	3.878(4)	
Au2−Au3	3.359(2)	0.28	Sr−M2[b]	3.852(3)		Sr2−Au2	3.516(2)	
In1−In2[a]	3.354(2)	0.48				Sr2−Au3	3.427(2)	
In−In3	3.474(2)	0.32				Sr2−In1[b]	3.853(4)	
In1−M1	3.015(3)	1.03/0.91				Sr2−In2	3.570(3)	
In1−M2	3.249(3)	0.71/0.66				Sr2−In3	3.587(2)	
In2−In2[a]	3.191(3)	0.68				Sr2−In4[b]	3.949(4)	

[a] Bonds between layers in Figure 1c for in $\mathrm{SrAu_{3.76(2)}In_{4.24}}$ and Figure 2b for $\mathrm{Sr_4Au_9In_{13}}$. [b] Distances between Sr and waist atoms in Figure 1c for $\mathrm{SrAu_3In_3}$ and Figure 2b for $\mathrm{Sr_4Au_9In_{13}}$. [c] As calculated for M1 = In, M2 = In. [d] M1 = Au, M2 = In.

Although the basic building unit of $\mathrm{SrAu_4In_4}$ has been defined geometrically as a 21-vertex $\mathrm{Sr@Au_9M_4In_8}$ (M = Au/In) polyhedron, the reasonably bonded neighbors in the Sr environment encompass only 6 Au, 8 In, and 4 M atoms (within 4.03 Å), which leads to practical coordination number 18. Three waist Au atoms are not well bonded to Sr ($d >$ 4.5 Å) and are not included in a reasonable coordination sphere for Sr, although in general, augmenting atoms about the waist in one prismatic unit are members of basal hexagons in the neighboring chains and vice versa. The distances from Sr to waist In and M atoms are in the modest range of 3.43 to 4.03 Å, whereas the Sr−Au/In/M distances within the hexagonal prisms show a somewhat narrower range of 3.35 to 3.81 Å.

In some contrast, Au−In/M bond distances exhibit a rather narrow range of 2.71 to 2.97 Å, suggesting that they are dominant. The lengths are comparable to those in $\mathrm{Ca_2Au_3In_4}$ (2.72–2.92 Å),[34] $\mathrm{AeAu_2In_2}$ (Ae = Sr, Ba) (2.69–2.93 Å),[16] $\mathrm{SrAu_3In_3}$ (2.71–2.92 Å),[25] and $\mathrm{Sr_2Au_3In_4}$ (2.71–2.92 Å).[24] There is only a single Au−Au contact here, a very long Au2−Au3 (3.359 (3) Å) which occurs between six-member rings in neighboring 21-vertex polyhedra, a weak bonding interaction according to electronic structure calculations (below). (The Pauling single bond metallic diameter is 2.68 Å.[35]) Without considering the mixed atom sites, there are several types of In−In contacts, including prism waist

---

(35) Pauling, L. *Nature of the Chemical Bond*, 3rd ed.; Cornell University Press: Ithaca, NY, 1960; p 403.

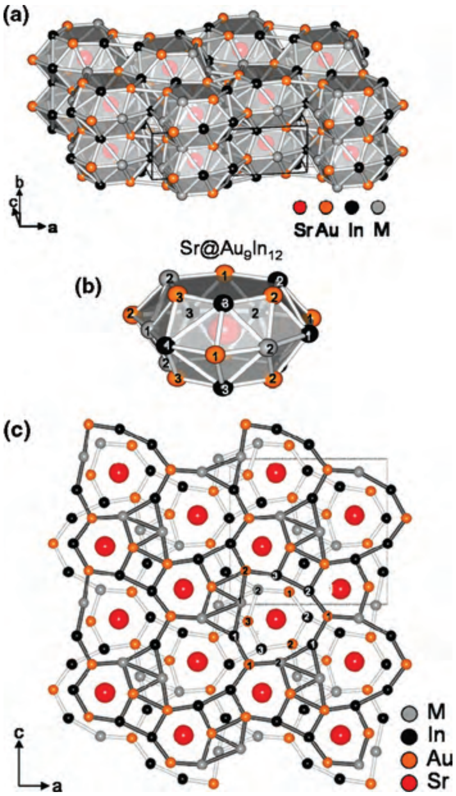

Figure 1. (a) General view of three-dimensional Au−In network in $SrAu_4In_4$ (*Pnma*). (b) A single basic building unit in $SrAu_4In_4$, the 21-vertex polyhedron centered by Sr, $Sr@Au_9M_4In_8$ (M = Au/In), (c) [010] view of the crystal structure of $SrAu_4In_4$. The atoms connected by black and gray lines are at $y = 1/4$ and $y = 3/4$, respectively. The connections between layers are not shown for clarity.

separations of In1−In2, 3.35 Å, In1−In3, 3.47 Å, In2−In2, 3.19 Å, and in the waist, In2−In3, 3.17 Å. All of these are comparable to those in other Au−In network compounds.[16,22,25,34] Their −ICOHP values are generally less than those for Au−In contacts (below).

Similarly, the crystal structure of $Sr_4Au_9In_{13}$ can be characterized in terms of a complex polyanion with Sr atoms encapsulated in augmented hexagonal prisms Figure 2a,b. However, in this case somewhat fewer network atoms per cation result in binding of three-fourths of the Sr in a complex $_{\infty}^{3}[Au_9In_{13}]^{8-}$ polyanion constructed from two basic units with more cluster sharing. The minority Sr1 is again encapsulated in a higher symmetry 6–9−6 unit $(\bar{6})$ built of six-membered Au−In rings plus a nine-member ring as the waist to give a 21-vertex $Sr@Au_9In_{12}$ polyhedron (Figure 3a). The second basic unit in the $Sr_4Au_9In_{13}$ structure is a complex trigonal polyhedron $Sr_3@Au_{18}In_{23}$ generated by fusion of three $Sr@Au_8In_{10}$ semicages. These cages can be derived from the former 21-vertex $Sr(1)@Au_9In_{12}$ polyhedron (Figure 3a), through removal of one Au2 atom and two In3 neighbors from the waist ring, which leaves two open pentagonal atomic faces 120° apart and perpendicular to the six-membered rings. Three such $Sr@Au_8In_{10}$ subunits then share pairs of [In2,In2,Au2,In1,Au2] pentagonal faces (as numbered in the new unit; Figure 3b) to create the trigonal $Sr_3@Au_{18}In_{23}$ polyhedron with $\bar{6}m2$ symmetry around the long (4.44 Å) common In2−In2 edge (In1−In1 in the parent cage). Along [001] (Figure 2b), each trefoil-like unit is bonded to three smaller $Sr@Au_9In_{12}$ neighboring units displaced by *c*/2 and vice versa, as seen in perspective in Figure 2a. The steps in the latter arise via the common waist prism atom junctions. Somewhat similar, complex $Ae_3@T_{18}In_{23}$ (T = late transition metal) building blocks are also found in $Sr(Eu)_2Au_3In_4$ and $Sr_2Pt_3In_4$ ($P\bar{6}2m$, $Hf_2Co_4P_3$ type) compounds.[24,34] However, the augmented prismatic construction in these is more complex; groups of three augmented hexagonal prisms share common edges and are separated by 5- and 6-fold prisms that share some inner prismatic atoms with the former groups. The formation of

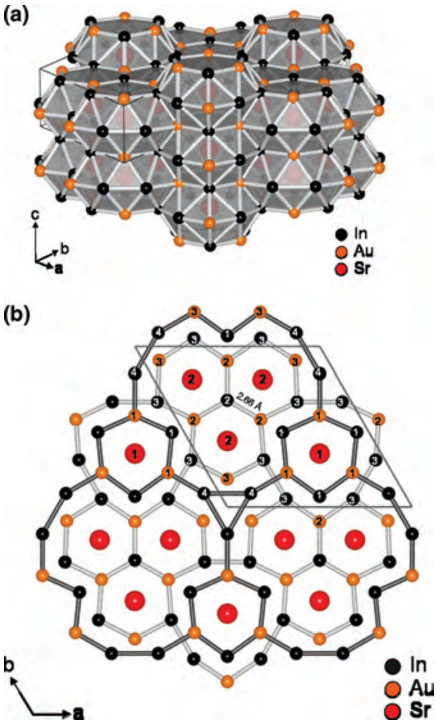

Figure 2. (a) General view of three-dimensional Au−In network in $Sr_4Au_9In_{13}$. (b) The [001] view of the crystal structure of $Sr_4Au_9In_{13}$. The atoms connected by black and gray lines are at $z = 0$ and $z = 1/2$, respectively, and the connections between layers are not shown for clarity.

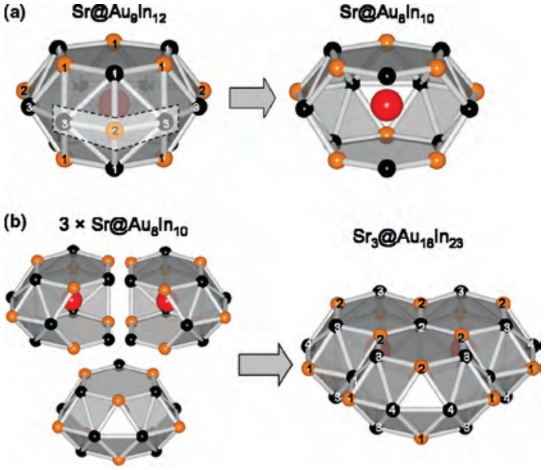

Figure 3. (a) The single basic building unit in $Sr_4Au_9In_{13}$, the 21-vertex polyhedron centered by Sr1, $Sr@Au_9In_{12}$, and its transformation to hypothetical semicage $Sr@Au_8In_{10}$. (b) Transformation of three $Sr@Au_8In_{10}$ semicages into the second building unit in $Sr_4Au_9In_3$, the trefoil-like $Sr_3@Au_{18}In_{23}$ centered by Sr2 atoms.

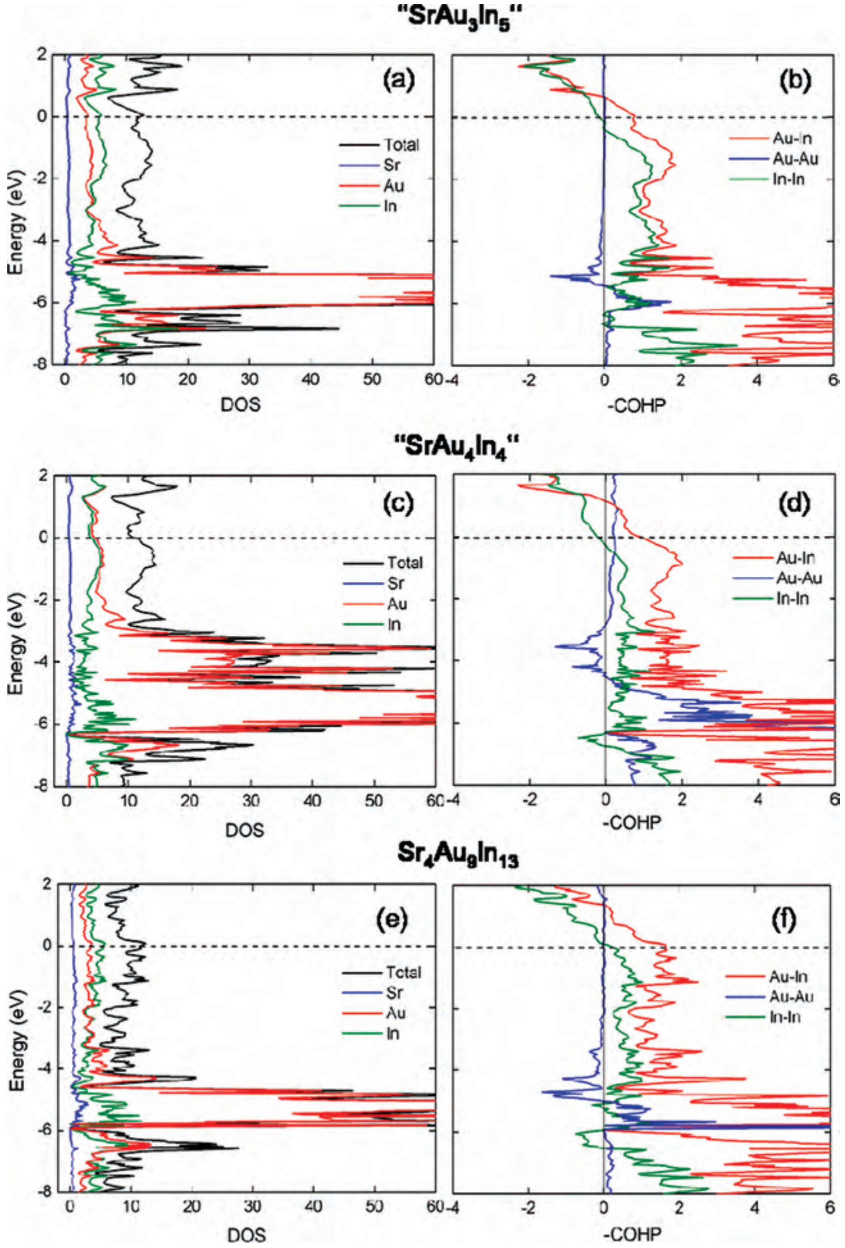

Figure 4. TB-LMTO-ASA electronic structure calculation results for the limiting compositions "$SrAu_3In_5$", "$SrAu_4In_4$", and for$Sr_4Au_9In_{13}$. (a, c, e) total DOS (black) and partial DOS curves for Sr (blue), Au (red), and In (green). (b, d, f) −COHP data for three different interactions: Au−In (red), Au−Au (blue), and In−In (green) (the last two are minor in frequency). The dashed lines denote the Fermi levels for the compositions indicated.

such complex structures depends on the stoichiometry and the relative Ae sizes and contents as well as on the flexibility of an anionic network and the optimal condensation results. With greater Ae contents, the waist augmentation of hexagonal prisms often can not reach nine or more atoms, and this leads to bonding between six-member rings in a variety of augmented ring systems of different sizes and interconnections.[16,22,24,25,36]

Strong heteroatomic bonding also occurs in $Sr_4Au_9In_{13}$, as expected. The Sr atoms occupy two crystallographically different sites (Figure 2b), and the anionic environment about Sr2 (Figure 3b) is practically the same as that in $Sr_2Au_3In_4$.[24] However, the environment of these Sr2 cations includes only 16 nearest neighbors, a higher value being unreachable because of the trefoil condensation brought on by the higher Sr content.

The three In2−Au2 distances of 2.66 Å in the center of the trefoil-like column (marked in Figure 3b) are now well less than the sum of Pauling's single bond radii (2.76 Å) and are also 0.03 Å shorter than the same in $Sr_2Au_3In_4$. The short bonds presumably arise from the relatively small number of bonded neighbors about each, In2 (x3) and Au2 (x5). The independent Sr1 atoms have a formal coordination number of 18 with 6 Au and 12 In neighbors. However, similar to the situation in $SrAu_4In_4$, the four Au1 in the waist of the trefoil-like polyhedron with Sr2−Au1 (waist) distances of 4.63 Å are bonded prismatic atoms only around Sr1, and likewise, the three Au2 atoms in the outer 9-ring about the

---

(36) Pöttgen, R.; Kotzyba, G.; Görlich, E. A.; Latka, K.; Dronskowski, R. *J. Solid State Chem.* **1998**, *141*, 352.

latter with Sr1−Au2 (waist) distances of 4.68 Å are effectively bonded only to Sr2 (d(Sr2−Au2) = 3.52 Å). The regular distribution of Au/In atoms in the nine-member waist about Sr1 ($\bar{6}$) (Figure 2b) contrasts with those about the augmented hexagonal prisms of Sr in $SrAu_4In_4$ (Figure 1c). All basal Au−In distances in the $\bar{6}$ $Sr@Au_9In_{12}$ polyhedron here are the same, 2.79 Å, the same as those around the waist. As in $SrAu_4In_4$ and number of other Au/In network compounds,[16,22,24,25,34,36] the short Au−In contacts in $Sr_4Au_9In_{13}$ are dominant and show strong bonding interactions. The strong Au−In interactions also correspond to the greater extremes in Mulliken electronegativity values:[37] Ae, 2.0–2.4 eV for Ca, Sr, Ba; In, 3.1 eV; Au, 5.8 eV, and are obviously very important factors in the formation of numerous compounds of this nature between the triels and gold or their neighbors.

Electronic Structure and Chemical Bonding. Because of the mixed atom sites in $SrAu_4In_4$, especially the almost 50:50 occupation of M1 site by Au/In, the LMTO-ASA calculations on the 1:8 phase were performed for two "ideal" compositions: "$SrAu_3In_5$" (M1 and M2 sites occupied by In) and "$SrAu_4In_4$" (M1 occupied by Au). The densities-of-states (DOS) calculated for both approximations as well as for $Sr_4Au_9In_{13}$ (Figure 4), exhibit broad bands and low densities around E_F, indicating metallic characteristics. The large and moderately wide peak around –5 eV in both "$SrAu_3In_5$" and $Sr_4Au_9In_{13}$ originates from the Au 5d orbitals. As expected, calculations for both compounds that exclude scalar relativistic effects narrow and move these bands to just below –6 eV. The occupation of M1 site in $SrAu_3In_5$ by pure Au leads to broadening of Au d energy range up to –3.5 eV. This reflects additional antibonding Au3−Au interactions around –4 eV (Table 3, Figure 4d,f), the same as has been observed in KAu_4In_6, $K_{1.76(6)}Au_6In_4$,[23] KAu_4Sn_6, and KAu_3Sn_3.[38] An increase of Au concentration in one of the approximations also brings fewer valence electrons into $SrAu_4In_4$, but the effect is relatively small as it shifts the E_F level from a small maximum on the total DOS (Figure 4a) to small minimum (Figure 4c) and makes the Au and In orbital contributions practically equal at E_F.

To compare the interactions between atoms, crystal orbital Hamilton population analyses (−COHP) were evaluated, as shown as a function of energy in Figure 4b,d,f for "$SrAu_3In_5$", "$SrAu_4In_4$", and $Sr_4Au_9In_{13}$, respectively, and as their integrands up to E_F in Table 3. In "$SrAu_3In_5$", strong bonding character is found for Au−In bonding, and both Au−Au and In−In bonds are practically optimized at E_F. Still more electrons populating In−In antibonding states might lead to structural instability of "$SrAu_4In_4$". On the other hand, Figure 4d suggests that fewer electrons could also cause instability. The substitution of some In by Au atoms in this comparison slightly increases antibonding character of In−In interactions at E_F. Although this substitution would also increase the amount of Au−Au bonding, and increases −COHP at E_F, the integrated (−ICOHP) values drop significantly (~0.2 eV/bond; Table 3). The overall bonding in both remains high. In general, the strong bonding characteristics of the heteroatomic Au−In interactions are dominant, corresponding to quite large −ICOHP values (> 1.2 eV/bond), and the relative frequencies of their occurrences are also logically large in many stable structure types compared with, for example, In−In and Au−Au or other bond types. The substantial polarity of the Au−In bonds, and thence their strong bonding (~ overlap populations), is very important in the present type of chemistry and in the Au−Tl and Au−Sn analogues, as well.

Acknowledgment. This research was supported by the Office of the Basic Energy Sciences, Materials Sciences Division, U.S. Department of Energy (DOE). The Ames Laboratory is operated for DOE by Iowa State University under Contract No. DE-AC02-07Ch11358.

Supporting Information Available: Comparison of observed and calculated powder patterns for $SrAu_{3.8}In_{4.2}$ and $Sr_4Au_9In_{13}$ and their refinement parameters in cif format. This material is available free of charge via the Internet at http://pubs.acs.org.

IC702145Y

---

(37) Pearson, R. G. *Inorg. Chem.* **1988**, *27*, 736.

(38) Li, B.; Corbett, J. D. *Inorg. Chem.* **2008**,in press.